Investigating of the Operation of a Railgun System with Laboratory Proportion

P. Sampaio Pereira[1], Mário Gatta[1,2], and M. Filomena Teodoro[1,3(✉)]

[1] CINAV, Center of Naval Research, Naval Academy, Portuguese Navy, 2810-001 Almada, Portugal

[2] Center of Philosophy of Sciences, Faculdade de Ciências, University of Lisbon, Lisbon 1749-016, Portugal

[3] CEMAT, Center for Computational and Stochastic Mathematics, Instituto Superior Técnico, Lisbon University, 1048-001 Lisboa, Portugal

maria.teodoro@tecnico.ulisboa.pt, mteodoro64@gmail.com

Abstract. In this document it is addressed the basic principles underlying the function of the railgun focusing in the electrodynamic questions. It is intended to acquire familiarity with this kind of weapon through the critical study of his functional principles. At first glance, the basic principle of operation of a railgun may seem simple in the light of the immediate application of the Lorenz force in a conductor driven by current. However, everything becomes more complicated in the case of a quick change of the involved parameters (transitional regime), which requires a more thorough analysis of current behavior, electric and magnetic fields, and all involved materials in the system.

This project also included the construction of two railguns, initially a smaller size one to gain familiarity with the system, and lastly a laboratory proportion one in which was performed and analyzed a number of tests with different materials and distinct projectile sizes. To better understand the process that involve the railgun process, an analysis in the time domain, of the spatial distribution of the electromagnetic field, electrical current and energy flow was performed. In the present paper, we describe the preliminary concepts about the studied weapon, the energy flow, complemented by a summary of the experimental work associated to the construction of the second railgun (in laboratory proportions) that allowed us to test distinct materials, forms and sizes.

Keywords: railgun · electric field · magnetic field

1 Introduction

The Lorentz force has been known for over two hundred years, but its application in a railgun was not immediate, and there were differing opinions on the subject. Only recently has its use been considered of great interest, and this interest has increased further with the construction of fully electric warships.

Since the last two decades of last century, the importance of magnetic acceleration weapons (MAGs) such as railgun has grown considerably. Applications are envisioned

© The Author(s), under exclusive license to Springer Nature Switzerland AG 2027
O. Gervasi et al. (Eds.): ICCSA 2026 Workshops, LNCS 16760, pp. 69–86, 2027.
https://doi.org/10.1007/978-3-032-30521-3_5

to replace traditional rapid acceleration systems in aircraft carriers, launching space platforms, welding, surface coating, and firing projectiles at hyper-velocity as a weapon system. The US Department of Defense, has been invested in the development of this technology greatly, e.g., in projects such as CHECMATE (Combat High Energy Capacitor Module Advanced Technology Experiment), whose main objective is the launch of ballistic missiles through a ground-based system.

With the end of the Cold War, in 1990, the enthusiasm surrounding this research reduced. With the 21st century and the fully electric ships of the U.S. Navy, the interest to lead to better-performing railguns to its new generation reborned. [1].

Railguns are almost as old as the concept of the coil gun (Gauss cannon or electromagnetic cannon). These accelerate a conductive electrical design that bridges a pair of current-carrying rails. The advantages that this technology brings to weapons systems include very high speeds (2 km/s or 61 $Mach$[1]), propellant-free ammunition, designs are much cheaper per firing and less bulky, greater safety in ammunition storage and the ability to use primary energy sources (electrical in tanks and ships) in a "parasitic" way instead of chemical expansion of gases that are toxic to humans.

Currently, the U.S. Navy is investing in the ultimate goal of achieving the capability of a weapon, with *mega joule* energy items, capable of making continuous fire at speeds exceeding 6 *Mach*, exceeding 200 nautical *miles* of range [1].

It is the interest of Portuguese Navy to pursue this technological evolution, evaluating the advantages of the adoption of this kind of weapon. In this document it is addressed the basic principles underlying the function of the railgun focusing in the electrodynamic questions. It is intended to acquire familiarity with this new kind of weapon through the critical study of his functional principles.

2 Basic Operation of a Railgun

It is currently widely accepted that a railgun projectile is accelerated by the Lorentz force. This force is described by equation (1) which describes the force on a particle with charge q moving with velocity v in the presence of an electric field E and a magnetic field B.

$$F = q\,[E + (v \times B)] \tag{1}$$

In the case of a railgun, the interacting field is magnetic, so it is possible to simply rewrite Equation (1) into (2) .

$$F = q\,(v \times B)\,. \tag{2}$$

The force element is written as $dF = idl \times B$ over a elemtent of flow idl.

2.1 Structure

The basic construction of a railgun is quite simple (see the Fig. 1), it only requires:

[1] 1 *Mach* is defined as the ratio between the speed of the object and the speed of sound.

- 2 metal conductors (which will serve as rails);
- 1 metal conductor that bridges the two conductors (the projectile itself or a projectile support (armor));
- 1 power supply (preferably direct current);
- 1 switch

Both types of current (direct and alternating) will accelerate the railgun projectile; however, pulsed current (direct or DC) is generally used for more powerful shots [2].

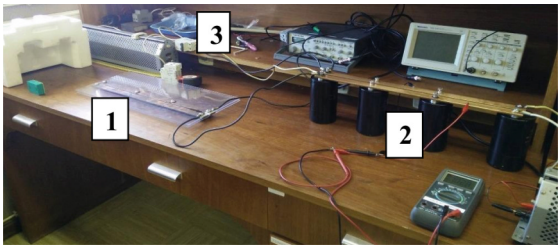

Fig. 1. Assembly of the second railgun built in this study. Legend: 1 – Parallel rails; 2 – Capacitor bank (Power Supply); 3 – Switch.

The architecture of a railgun consists of two metallic conductors that serve as rails, and an electrically conductive projectile that closes the circuit, thus connecting the two rails. The current flows through one rail, passes through the projectile, and returns to the source through the other rail, creating a magnetic field (see the Fig. 2).

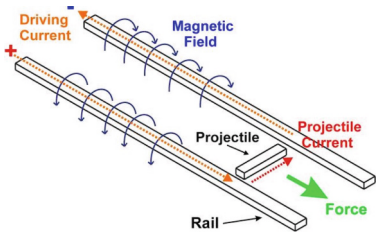

Fig. 2. Diagram of the interaction between the magnetic field B and the current flowing in the projectile. Source [3].

The magnetic field generates a Lorentz force, pointing outwards, in all components of this current loop. Railguns take advantage of this phenomenon to accelerate the projectile out of the rails.

The Lorentz force equation in its original form can be complex to work with in practical cases like railguns. To simplify these cases, equation (2) was rewritten as a function of the current I and the inductance gradient $L^{'}$. The derivation of equation (3) from equation (2) and the calculation of $L^{'}$ from the rail geometry can be found in [1] and it is given by

$$F = \frac{L' I^2}{2}. \tag{3}$$

The inductance gradient is given by Eq. (4):

$$L' = \frac{\mu_0 I^2}{2\pi} ln\left(\frac{d-r}{r} Y\right). \tag{4}$$

where d represents the length of the rails and r the distance between them.

3 Model

The assembly of a conventional railgun is simple. The rails must be parallel and the projectile in the middle of the rails and in contact with them, so that the projectile closes the electrical contact, as shown in Fig. 3, on the right.



Fig. 3. Left - prototype tested on the destroyer ship "Zumwalt" (US Navy). Right, scheme of a conventional railgun that uses a sabot to close the electrical contact.

A high-voltage power supply (typically banks of high-voltage and high-capacitance capacitors) is needed to rapidly discharge the circuit, accelerating the projectile.

The objects that railguns fire are called projectiles or armatures.

When the goal is to hit the target with the complete object that was fired, it is called a projectile; if a sabot is used to close the electrical contacts, the assembly (projectile and sabot) is called an armature. Currently, in railgun weapon systems, a conductive sabot is used to make contact with the rails. As soon as the assembly leaves the rails, the sabot is separated from the projectile due to its less aerodynamic shape.

4 Problems in Railgun System

The fact that certain Navies are ready to use this type of weaponry means that railguns, which were once unreliable and had a short lifespan, have overcome or at least reduced the problem of rail damage. This damage can take many forms due to the extreme conditions to which they are exposed.

High temperatures, metal-to-metal friction, high projectile speeds are just some of the conditions that the rails will have to withstand for the longevity of a railgun to be viable for military use.

4.1 Excavation or Gouging

Excavation occurs due to high sliding speeds, as happens in missile and railgun tracks. This effect takes the form of craters similar to a drop of water (see Fig. 4, left), and occurs above a limiting speed value depending on the friction and properties of the involved materials [4]. Excavation is a problem for two reasons: on the one hand, this process generates a very high dynamic stress that can lead to failures in both the rails and the projectile of a railgun; on the other hand, the use of material already with this effect can lead to areas of non-contact with the armor. Most importantly, when excavation occurs, a tremendous force is exerted on the armor in the opposite direction of movement, substantially reducing the performance of the railgun. Excavation became a problem in railguns when they began to be built with solid armor accelerators in 1980. In the construction of a railgun, the most important criterion in choosing the material for rails is their high electrical conductivity. Copper for rails and aluminum for armor are the most common choices. Replacing the rails with aluminum and the projectile with copper would substantially reduce this effect, however, the yield would inevitably drop because aluminum is a worse conductor than copper. A copper projectile is not the best choice because it is a denser material than aluminum, making it heavier [5].



Fig. 4. Left: Excavation in copper rails. The black arrow indicates the direction of movement. Source [4]. Center: Damage inflicted by the bows on the railgun built by Power Labs. Source [6]. Right: Example of an aluminum tank verified on the Railgun *MK*1.1. Source [7].

4.2 Current Arcs or Arcing

Generally, arcs occur when the contacts between the rails and the projectile are not perfect. During the projectile's path along the rails, it has been recorded that half of its mass is lost due to heating and friction at high speeds ([5]). When there is a small gap between the projectile and the rails, and if the electromagnetic field is strong enough, arcs are formed and the current travels through the air until it reaches the projectile. These current jumps through the air decrease the efficiency of the railgun because the current travels through areas of very high resistance (air), losing a large part of its energy in the formation of current arcs. The damage caused by the arcs is visible and deteriorating to the rails, as can be seen in Fig. 4, on left.

4.3 Deposits Excess

Deposition occurs during projectile firing when it heats up due to high speeds and friction, leaving part of its mass in a liquid state on the rails (see Fig. 4, on right). This layer of liquid aluminum is beneficial because it acts as a lubricant during firing [5]. Subsequently, these aluminum deposits cool and solidify, becoming very irregular, flaky, and porous, reducing the performance of subsequent shots. Accuracy in the distance between rails is crucial in a railgun because any disturbance

in the caliber results in loss of electrical contact, less efficiency, and decreased longevity of the weapon. Therefore, one way to reduce the amount of deposits is to improve the electrical contact between the rails and the projectile, so that there is a uniform zone with compatible sections, avoiding as much as possible areas of constriction for the current.

5 Power Supplies

The low efficiency level of a railgun is practically inevitable. Even using techniques to improve the weapon's performance, such as the use of electrically conductive lubricant, low electrical resistance rails, and projectile pre-acceleration, we still have efficiencies below 40%, and in the best cases it is possible to reach up to 66% [8,9].

Due to the low yields, to achieve speeds greater than Mach 6, such as the new weapon developed by the US Navy [10], enormous amounts of stored energy (on the order of MJ) are needed, which are subsequently released almost instantaneously in the projectile. Typically, capacitor banks are used to store electrical energy. To release all the stored energy, switching mechanisms are used that can handle high currents. The most common components are thyristors or spark gap switches. The spark gap switch are less common. They consist of an assembly with two conductive electrodes separated by a space filled with air or gas. This is designed to allow an electric spark to pass between the conductors when the voltage difference reaches the breakdown voltage of the gas in that space [11]. Table 1 compares different railgun configurations already tested, as well as the voltage of the capacitors and activation mode of the projectile [6,12,13].

Table 1. Scale of stored energy in different railgun designs.

Railgun	Number of capacitors	Stored Energy	Activation Mode
1º Proj	3 (385 V)	500J	None
2º Proj	13 (400 V)	11 kJ	None
Powerlabs 2.0	32 (450 V)	20 kJ	None
Cal Poly Mk 1.0	16 (450 V)	16 kJ	None
Cal Poly Mk1.1	16 (450 V)	16 kJ	Thyristors
Cal Poly Mk 2.0	2 (9 kV)	67 kJ	*Spark Gap Switch*
GA Blitzer	Unknown	2 MJ	Solid-State Switch
GA/US *Navy*	>200 (11kV)	9 MJ	Solid-State Switch
BAE/*Navy*	29 bench (11kV)	>32 MJ	Unknown

6 Charging and Discharging Capacitors

6.1 Charging Phase

The energy required for a railgun to operate is stored in the capacitors, in the form of electrical energy in the field between the plates. It is important to know, rigorously, their behavior during the discharge phase, because in addition to the typical capacitor discharge curve, there are other variables depending on time, such as electrical resistance and Lorentz force.

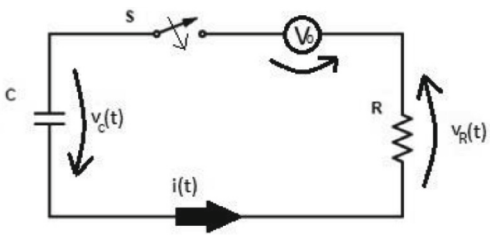

Fig. 5. Diagram of an RC circuit.

The charging circuit of a railgun can be approached as a circuit that consists of a resistor **R**, a capacitor**C**, and a source **V**, in series. This circuit is known as an **RC** circuit, as shown in the Fig. 5.

The charging of a capacitor in an *RC* circuit is described by the voltage across its terminals, $v_c(t)$, and $i(t)$, the current flowing through the circuit.

$$v_c(t) = V_o\left(1 - e^{-\frac{t}{RC}}\right), \tag{5}$$

$$i(t) = I_o e^{-t/RC}. \tag{6}$$

$$v_R(t) = Ri(t) = R\frac{dq_c(t)}{dt}, \tag{7}$$

$$v_c(t) = \frac{1}{C}q_c(t), \tag{8}$$

$$-v_0 + v_R(t) + v_c(t) = 0 \rightarrow \tag{9}$$

$$\rightarrow -v_0 + R\frac{dq(t)}{dt} + \frac{1}{C}q(t) = 0 \rightarrow \tag{10}$$

$$\rightarrow \frac{dq(t)}{dt} + \frac{1}{RC}q(t) = \frac{1}{R}v_0, \tag{11}$$

Equation (5) models the voltage across the capacitor as a function of time after the switch *s* is closed, $v_c(t)$ is the source voltage, *R* is the resistance value in the circuit, and *C* is the capacitance of the capacitor *C*. Equation (6) represents the current $I(t)$ as a function of time *t* and *I(0)* the peak current, with $I(0) = \frac{V_0}{R}$. These equations can be obtained by solving the differential equation of an *RC* circuit under load, as we know from electrical engineering, $q_c(t)$ represents the charge on the capacitor. After closing the switch, we get an ODE (11) as follows from the circuit under load, with the Eq. (9).

$$\text{Homogeneous equation:} \quad \rightarrow \frac{dq_h(t)}{dt} + \frac{1}{RC}dq_h(t) = 0 \rightarrow \\ \rightarrow q_h(t) = ke^{-\frac{t}{RC}}, \tag{12}$$

$$\begin{array}{c}\text{Complete equation:} \qquad \rightarrow q(t) = q_p(t) \rightarrow \\ = \text{constant} = 0 + \frac{1}{RC} q_p = \frac{1}{R} v_0 \rightarrow q_p = C v_0.\end{array} \tag{13}$$

$$\boxed{q(t) = k e^{-\frac{t}{RC}} + C v_0}, \tag{14}$$

for $t = 0 \rightarrow q(t = 0) = 0 \rightarrow 0 = k e^{\frac{0}{RC}} + C v_0 \rightarrow \boxed{k = -C v_0,}$

$$\boxed{q(t) = -C v_0 e^{-\frac{t}{RC}} + C v_0} \rightarrow \tag{15}$$

$$\rightarrow \boxed{q_c(t) = C v_0 \left(1 - e^{-\frac{t}{RC}}\right),} \tag{16}$$

once $q_c(t) = C v_c(t)$, we obtain $\qquad \boxed{v_c(t) = v_0 \left(1 - e^{-\frac{t}{RC}}\right)}$, (17)

given that $i(t) = \frac{dq_c(t)}{dt}$, we get $\qquad i(t) = 0 - C v_0 e^{-\frac{t}{RC}} \left(-\frac{1}{RC}\right)$,

$$i(t) = \frac{v_0}{R} e^{-t/RC} = I_0 e^{-t/RC}, \tag{18}$$

To solve the ODE (11) we need to get the general solution of the homogeneous EDO associate to Eq. (11) and a particular solution of the complete Eq. (11).

The general solution to the given ordinary differential equation is the sum of solutions (12) and (13), resulting in Eq. (16) which relates equalities (17) and (18), confirming Eqs. (5) and (6). The solutions given by formulae (17) and (18) are displayed in Fig. 6.

In the first phase of this work, three capacitors were used, each with $2200\mu F$ and a maximum voltage of $385V$. With these capacitors, a parallel capacitor bank was assembled, that is, the total capacitance becomes the sum of the 3 capacitances, maintaining the voltage, $C_{total} = C_1 + C_2 + C_3$. The first problem that arose was the charging of the capacitors, since it is necessary to use a source of at least 385 V for the capacitors to get close to that value. This equipment is not commonly found in the laboratory and is perhaps expensive. Therefore, a high-voltage capacitor charging circuit was acquired, whose function is to obtain an adjustable output voltage from this circuit, between the 250 V and 420 V. The complete charging circuit is represented in the diagram on left in Fig. 7.

This charging circuit is powered by a **DC** voltage of $3.2V$ to $6V$. Before testing the right loop, calculations were made to ensure that the energy dissipated in resistor R_1 did not exceed its limit, and consequently melt or damage the rest of the components. It is known that the dissipated power is given by $P = VI$ (W ou Js_{-1}), and rewriting the current as $I = V/R$, we obtain $P = V^2/R$.

Generally, in the case of laboratory resistors, these dissipate up to $1W$. We can then express the value of R_1 so that it does not exceed its dissipation limit, thus obtaining the value of $R_1 = 160k\Omega$.

Charging Time. With the charging equations, the voltage across the capacitor at each instant is easily known, as well as the maximum current that will flow through the circuit when switch 2 is closed. In Equation (4.2), the maximum current value is reached at time $t = 0$, since the solution is simply equal to the peak current, 0, (see Fig. 4.2). It is also known that it is given by $I_0 = \frac{V_0}{R}$, so if $R_1 = 160k\Omega$ and $V_0 = 420V$, the maximum current value that flows through

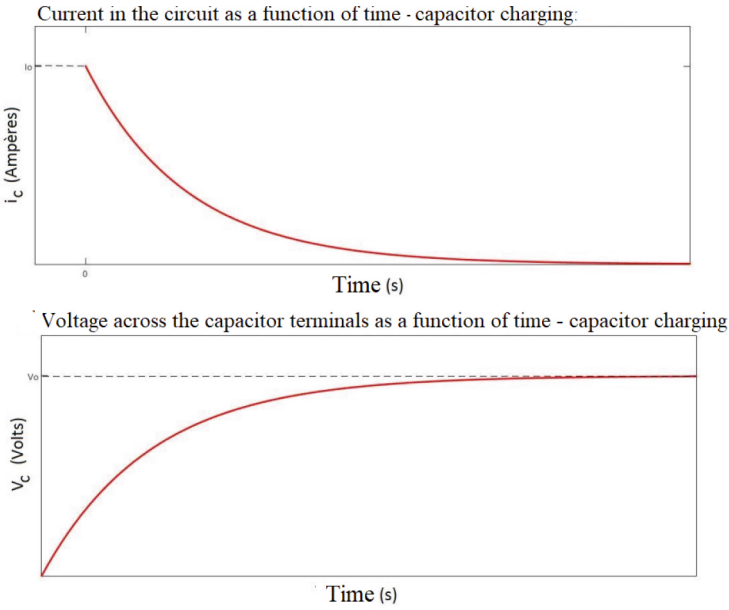

Fig. 6. Current and voltage curves as a function of time, respectively.

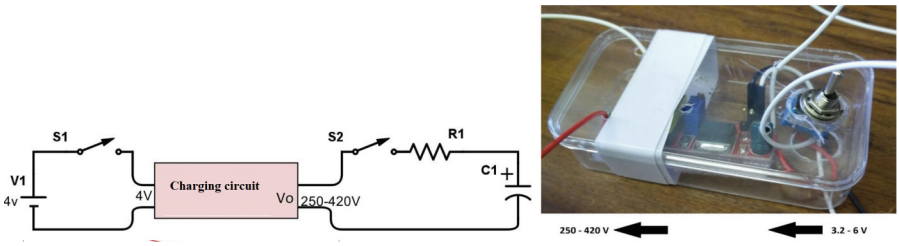

Fig. 7. Left - Charging circuit scheme. Right - Charging circuit purchased. Subsequently, this circuit was adapted and placed inside the plastic box, and a switch was added for safety purposes.

the right loop is $2.63mA$. To get an idea of how long it takes a capacitor to charge, Equation (4.1) was used. For example, to charge a capacitor at $200V$ using a $V = 400V$ and $R = 160k\Omega$, simply solve Equation (5) in order to time. Therefore, a capacitor takes about 4 min and 20 s to charge to $200V$. Of course, there is still room to reduce the charging time of the capacitors. To do this, simply lower the resistance value, however, without exceeding its power dissipation limit. A rheostat with $R = 360\Omega$ was used, which can handle currents up to $10A$. It was replaced by resistor R_1 of $160k\Omega$, thus resulting in a charging of the 3 capacitors to $200V$ in 1.54 s, theoretically. This significant improvement made it possible to carry out several laboratory tests without the constraint of the charging time.

Despite the agreement of the previous image (Fig. 8 left) with the theoretical charging curves, the actual charging times were different from the theoretical ones, namely much longer. As can be seen in Fig. 8, the charging time of 3 capacitors at $200V$ was approximately 120 seconds. After

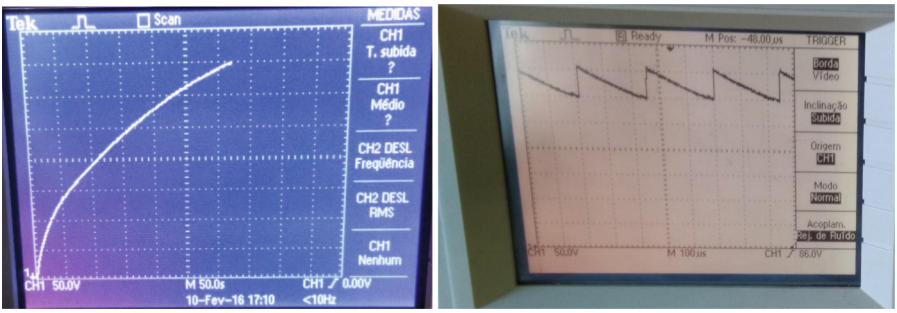

Fig. 8. Left - Image taken from the oscilloscope during capacitor charging. This image is consistent with the expected theoretical curve in Eq. (5) and Fig. 6. Right - Signal at the output of the capacitor charging circuit measured on an oscilloscope.

investigating the charging circuit, it was noted that the connections between the terminals of the charging circuit and the capacitors were not the best; some contacts had dirt and even some rust, as they were quite old. These factors contributed to an increase in the overall resistance of the right-hand loop (see Fig. 8, right), and consequently lower current values and longer charging time. After cleaning the contacts, the charging time improved slightly, however, far from the theoretical values ($1.54s$). Finally, it was decided to connect the terminals of the charging circuit to an oscilloscope to see what type of signal was entering the capacitors, and the image at bottom of Fig. 8 was observed. As can be observed, we are not dealing with a clean DC signal, as one would expect, but rather a signal that oscillates up to $50V$ of voltage. This phenomenon is called *ripple* voltage.

This *ripple* is derived from the incomplete suppression of an alternating current, created in the charging circuit, typically associated with chargers that use current rectifiers, as is the case here. The operating principle of a charger that uses current rectifiers can be described by the diagram displayed in Fig. 9.

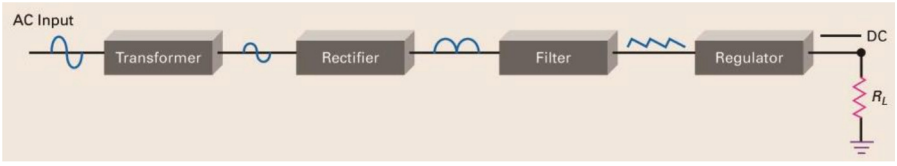

Fig. 9. Diagram of the operation of a charger based on rectifiers. Source [14].

One of the major steps that the railgun project will need is effectively a power supply specifically designed for charging capacitors at $400V$, with the capacity to charge a bank of capacitors consisting of 10 capacitors of $6600\mu F$.

6.2 Discharge Phase

The most important phase of a railgun is the discharge, as this is where all the weapon's kinematics take place. The discharge circuit can be represented by the scheme in Fig. 10.

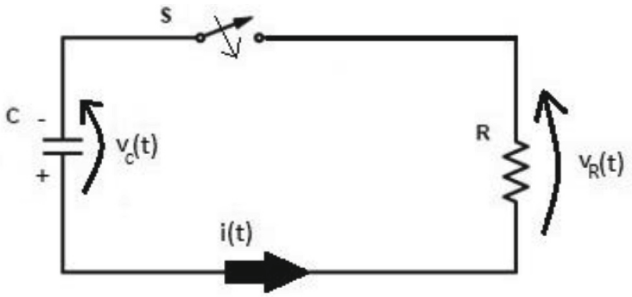

Fig. 10. Railgun discharge circuit.

Similar to the charging phase, the solutions can be obtained from the first-order differential equation of a discharging RC circuit (Eq. 21). This EDO is deduced applying the Kirchhoff, obtaining the relation defined by Equation (19). Ssolving Equation (21), aftr some calculations that follows we obtain the two solutions of interest: Equations (25) and (26).

$$-v_C(t)+v_R(t)=0 \tag{19}$$

with $v_c(t)=\frac{1}{C}q_c(t)$, $v_R(t)=Ri(t)$ and $i(t)=-\frac{dq_c(t)}{dt}$, so :

$$-\frac{q_c(t)}{C}+Ri(t)=0\rightarrow-\frac{q_c(t)}{C}+R\frac{-dq_c(t)}{dt}=0\rightarrow \tag{20}$$

$$\rightarrow\frac{q_c(t)}{C}+R\frac{dq_c(t)}{dt}=0, \tag{21}$$

$$\frac{dq_c(t)}{dt}+\frac{1}{RC}q_c(t)=0\rightarrow\boxed{q_c(t)=ke^{-\frac{t}{RC}}}, \tag{22}$$

in $t=0$ we have $v_c(t=0)=v_{c_0}$, also $q_c(t=0)=Cv_{c_0}=ke^0=k\rightarrow\boxed{k=Cv_{c_0}}$
so:

$$q_c(t\geq0)=Cv_{c_0}e^{-\frac{t}{RC}}\rightarrow \tag{23}$$

$$\rightarrow v_c(t\geq0)=\frac{1}{C}q_c(t\geq0)\rightarrow \tag{24}$$

$$\rightarrow v_c(t\geq0)=v_{c_0}e^{-\frac{t}{RC}}. \tag{25}$$

By definition, $i(t)=-\frac{dq_c(t)}{dt}=-\frac{d}{dt}\left(Cv_{c_0}e^{-\frac{t}{RC}}\right)=Cv_{c_0}e^{-\frac{t}{RC}}\frac{1}{RC}$
Simplifying, we obtain:

$$\boxed{i(t)=\frac{v_{c_0}}{R}e^{-\frac{t}{RC}},} \tag{26}$$

$$v_c(t)=v_{c_0}e^{-t/RC}, \tag{27}$$

$$I(t)=I_oe^{-t/RC}, \tag{28}$$

Summarizing, the solutions that describe the discharge curves of the capacitors are given by formulas (27) and (28), with $I_0=V_0/R$whose graphical representation is made in Fig. 11.

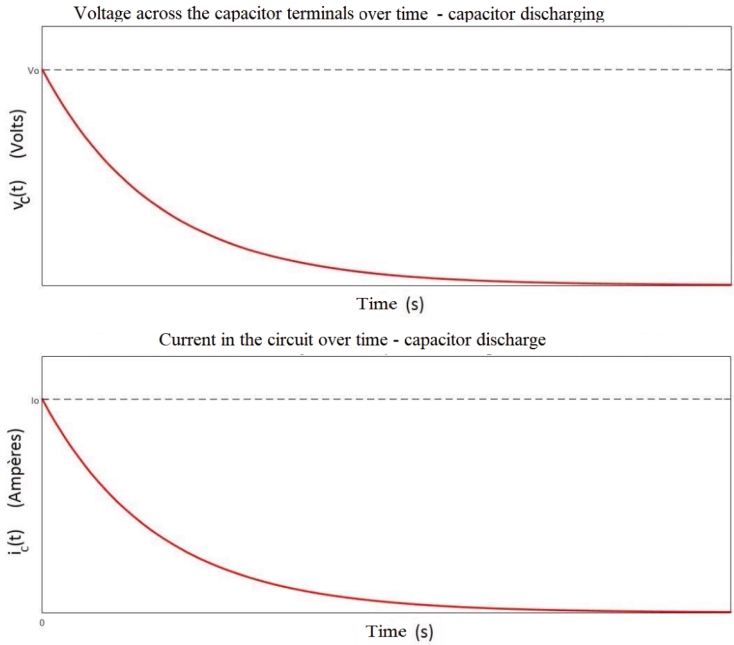

Fig. 11. Discharge curves of capacitors, above the voltage curve as a function of time Equation, below the current curve as a function of time Equation.

This is the typical behavior of a capacitor; however, for our system, we have to complete the discharge equations to make them as similar as possible to reality. To do this, it is necessary to analyze the behavior of the electrical resistance of the system.

7 Experimental Part

At first glance, the basic principle of operation of a railgun may seem simple in the light of the immediate application of the Lorenz force in a conductor driven by current. However, everything becomes more complicated in the case of a rapid change of the parameters involved (transitional regime), which requires a more thorough analysis of current behavior, electric and magnetic fields, and all materials involved in this system. This part of study can be found in [15], where the theoretical part is developed. In this paper an analysis in the time domain, of the spatial distribution of the energy flow was performed shortly. Now, the work is complemented by the experimental part. This project also involved the construction of two railguns, initially a smaller size one to gain familiarity with the system, which is described in [16]. Lastly, a laboratory proportion one in which was performed and analyzed a number of tests with different materials and projectile sizes that is presented here.

7.1 Railgun with Copper Rails

When building a railgun, the first concern must be energy storage, optimizing it and designing the rail architecture (length of the rails) as a function of the capacitor bank discharge time.

Ideally, the rails should have a length such that the instant the projectile leaves the rails coincides with the instant the capacitors are discharged.

We describe the construction and experimentation of one of the railguns used in this study. Due to a lack of experience in handling high currents, a smaller and simpler model of a railgun was first built in order to gain familiarity with this type of system: the railgun with aluminum rails.

The first railgun, built for this study, consisted of: a laboratory DC power supply, the capacitor charging circuit (discussed in the fourth chapter), three $2200\mu F/385V$ capacitors, two aluminum rails, and spherical steel projectiles of three different diameters. The detailed description of the results associated to the first railgun can be found in [16].

In the analysis of the slow-motion images of the shots, although the demonstration of the Lorentz force is quite visible, the efficiency of the first railgun was very low. The existence of sparks flying after the discharge and the formation of arcs were the causes of the low efficiency, as the waste the energy that should be used to accelerate the projectile. That project worked with spheres as projectiles, it was suspected that such geometric shape was not ideal for obtaining good electrical contact. The contact sections must be compatible, that is, if the rails are rectangular in section, the projectile must also have flat sections. To lower the electrical resistance and, consequently, increase the current in the system, copper rails were used in the actual project since they have a higher electrical conductivity. The projectile pre-acceleration system was adapted because we no longer have spheres as projectiles, this ramp will cease to function. The second railgun project are made of copper and had a rectangular cross-section, thus, we improved not only the contact between rails and projectile (both have flat cross-sections) but also the electrical resistance of the projectile due to the greater conductivity of copper compared to steel With these changes, it is expected that efficiency will increase, making the Lorentz force effect more visible, and also that the railgun will be capable of multiple shots without the need for rail repair.

For the construction of the second railgun, copper rails were used. The choice of this material is due to its high electrical conductivity, $5.91 \times 10^{-9}(\Omega m)^{-1}$, almost twice as good as aluminum, $3.63 \times 10^{-9}(\Omega m)^{-1}$, used previously. It was decided to use rails with $50cm$ each, as this length allows a complete discharge of the $106600\mu F$ capacitors in parallel, according to the study done in the fourth chapter. It was agreed that the spacing between rails would be $4mm$ (which will also be the width of the projectiles), however, adjustable if projectiles with different dimensions are to be used. Projectiles with a width of $4mm$ and different lengths were used in order to perform various tests and determine which one yields the best results (see Fig. 12).

To reduce the danger of using the railgun, an insulating section was created at the beginning of the rails, in order to allow the projectile to be placed inside the rails safely.

Acrylic was used as support for the structure instead of wood, which was used previously. A sheet of acrylic was placed on top and another underneath, with the rails in the middle of the sheets. This prevents pieces of molten metal from flying towards the operator, as happened in the previous project. Both the acrylic and the rails are fixed by 8 screws and 8 nuts located asymmetrically, preventing the rails from separating during firing due to the Lorentz force that also manifests itself between these.

7.2 Details of the Shooting

Four sets of tests were performed with the following initial conditions:

- With 1 capacitor bank of 3 capacitors at 350 V of 2200 μF, without lubricant;
- With 1 capacitor bank of 3 capacitors at 200 V of 2200 μF, with graphite on the rails;
- With 1 capacitor bank of 4 capacitors at 200 V of 6600 μF, without lubricant;
- With 1 capacitor bank of 2 capacitors at 380 V of 6600 μF, with a silver-based grease.

In this second railgun, another form of projectile pre-acceleration was tested.

A small slingshot was constructed, consisting of a plastic tube, a balloon, a thin rubber band, and a thin bamboo stick. In the first set of tests, 3 shots were fired, one successfully, hitting a styrofoam plate that was $20cm$ from the end of the rails, but two misfires occurred in the last shots. After the misfire, it was found that there was already some wear on the rails. In order to reduce wear on the rails, in the second set of tests, graphite was used as a conductive lubricant on the rails and projectile, similar to that used by Pavlov [5]. To apply the surface layer of graphite, a conventional pencil was used, scraping it against the surface of the rails. In the 3 shots performed, two were successfully recorded (see Fig. 12), similar to the shots in the first set of tests.



Fig. 12. Left - Comparison of the length of various copper projectiles. From top to bottom, length $L = 2.0cm$, $L = 1.8cm$ and $L = 0.6cm$. Right -Frame during the first shot of the second round of testing.

The recorded misfire occurred because the projectile welded to the rails in the first moments of discharge, resulting in considerable excavation in the rails. The major difference observed from the first set of shots to the second was the reduction in rail wear, which is an improvement in the longevity of the material. For the third round of tests, we already had the new 6600 $\mu F/400V$ capacitors available. Four capacitors were mounted in parallel, as shown in the figure. With this setup, the Lorentz force will be of the same intensity as in the second set of tests (see Eq. 3), since we are using the same voltage (and consequently the same initial current[2], on the order of tens of thousands *Amperes*), however, this force will be exerted for a longer time, namely, four times longer due to the increased capacitance of the new capacitor bank (Fig. 13).



Fig. 13. Capacitor assembly used in the third and fourth rounds of railgun testing.

[2] Since during the discharge of capacitors, we have $I_0 = \frac{V_0}{R}$ and $I(t) = I_0 e^{-\frac{t}{RC}}$.

Three shots were fired, none of them successful, resulting in a more pronounced excavation than in previous cases. It should be noted that in this case we had four times more energy involved in the discharge, which caused the projectile to heat up even more and weld itself to the rails, damaging both in such a way that it was imperative to carry out repairs to the rail, eliminating the irregularities caused by the shots.

Analyzing the firing failures of the previous tests, it was concluded that the problem was possibly at the level of friction that the projectile encountered while sliding between the rails. We tried to find a lubricant (similar to graphite) that would reduce friction but not increase electrical resistance. We were advised by a specialist to use a silver39-based grease, which a prior met the aforementioned requirements. After applying the lubricant to the rails , it was noted that the mass was somewhat dense, which could increase friction instead of decreasing it.

For the final round of tests, in order to give the projectile an initial velocity and prevent it from sticking to the rails, another method was used to provide initial propulsion to the projectile. Compressed air similar to that used for cleaning hardware in electronics was employed. Instead of 4 capacitors in parallel, it was decided to use 2 capacitors in parallel, which allowed for a reduction in the charging time of the capacitors and the use of a higher voltage, 380 V. Three shots were made with the applied lubricant, and similar to the tests in the previous round, they resulted in misfires. The projectile ended up sticking to the rails at the beginning of the discharge, and it was observed that the damage done to the rails was even more severe than in previous cases (see Fig. 14), both in terms of rail deformation and the excavation caused by the projectile, ultimately rendering the rails unusable for future tests (Table 2).

Table 2. Data from the results obtained after the four sets of railgun shots.

	Voltage	Capacitance	successfull shoots	unsuccessfull shoots
No lubricant	350 V	6600 µF	1	2
Graphite	250 V	6600 µF	2	1
No lubricant	200 V	26 400 µF	0	3
lubricating grease (silver)	380 V	12 000 µF	0	3

7.3 System Damage

Two types of damage were recorded in the system, mentioned in the first chapter: the excavation in the rails and the effects of current arcs on the projectiles. The excavation in the rails became increasingly greater as the amount of energy in the capacitors increased, being more visible in the last round of firing. The damage caused by the excavation led to the rails becoming unusable after 12 shots, as can be seen in the Fig. 14.

The lubricant that yielded the best results was graphite, both in terms of material protection and weapon effectiveness (fewer misfires). Initially, it was thought that grease would yield better results, however, due to its high density and viscosity, it ended up further increasing the coefficient



Fig. 14. Damage to the rails after the last round of shots. Damage caused by the excavation effect of the projectile on the rails. Damage caused by arcing currents in the initial zone (right) of the projectile. Note the similarity of the wear pattern to that found on other railguns.

of friction between the projectile and the rails, leading to misfires. Despite the material being of high quality, it was not the most appropriate considering the reduced dimensions of the railgun. It should be noted that graphite is much less expensive (common in traditional graphite pencils) and easier to apply compared to grease, which requires using the precautions recommended by the manufacturers for its application.

After several shots, it was concluded that the larger projectile, obtained the best results. The smaller, lighter projectiles ended up generating the recorded misfires. The larger projectile, perhaps because it has greater inertia, resists the initial friction between the rails and it projects itself better. Due to the wear of the projectile, it is not advisable to use it for more than three shots, since the deposits accumulated on the projectile, in addition to adding irregularities, have low conductivity. When the irregularities in the projectile are removed, strictly speaking, we are reducing the dimensions of the projectile. These small changes are enough to create a slight misalignment between the rails and the projectile that could increase the probability of excavation and current arcs.

At the capacitor level, numerous discharge tests were performed (more than 30 discharges, in addition to the recorded discharges) for a rheostat, which functioned as a load, with no signs of wear on the capacitors or decrease in their performance.

8 Discussion and Final Remarks

Major Constraints

There were two major constraints that limited the analysis to the obtained results. The first was the absence of equipment to measure the projectile's velocity at the muzzle of the rails. With this measurement, it would be possible to have a general idea of the weapon's performance, comparing velocities with different initial conditions, and also to compare the practical results with the theoretically predicted results. The second limitation was the lack of a clamp or hook anemeter, which would allow quantifying the current present during firing; if we had this measurement, it would be possible to predict the theoretical velocity of the projectile, which, when compared with the actual velocity, would give the efficiency index η of the weapon.

Rails Size

An important conclusion drawn was regarding the size of the rails, where it was verified that the discharge of the capacitors was carried out only with the projectile in the first third of the tracks, that is, the rest of the track length contributed only with friction. Although the total capacitance of an assembly of $106600\mu F$. capacitors in parallel, which would extend the discharge of the bank, was not used, it is predicted that half the current length, $L_{rail} = 25cm$, would be sufficient to complete the discharge of the capacitor bank proposed.

Capacitor Bank and Power Supply

In the tests performed, only four of ten $6600\mu F$ capacitors were used, as the charging circuit could not handle such high currents. Furthermore, when testing the charging of six capacitors in parallel, some of the circuit components melted and smoke was released. This will be a problem that will inevitably have to be addressed in future designs of this railgun, as we aim to charge the capacitor bank proposed above (ten capacitors). It should also be noted that the development of a power supply designed for the fast charging (less than 60 s) of a capacitor bank at a voltage of 1200 V with a capacitance of $26400\mu F$.

Regarding the capacitor bank configuration, with the proposed change to the rails (reduction to 25 cm in length), it is proposed, similar to the discussion in the fourth chapter, that tests be carried out with a configuration of a bank consisting of three secondary banks mounted in series, in which each secondary bank has four capacitors connected in parallel, resulting in a current of 19 kJ with a discharge time of $9.6\mu s$, similar to what was done in the Powerlabs railgun [6]. With this configuration, an optimization between the relationship between "discharge time" and "available energy" is expected.

Projectile Dimensions

Although several projectile dimensions were tested for the railgun, it was not conclusive what the optimal projectile length would be; however, it was confirmed that the largest dimension, $L = 2.0cm$, obtained better results compared to the smaller ones. It is encouraged that other materials be tested for the constitution of the projectile, particularly aluminum, which presents itself as a strong candidate due to its electrical conductivity, low density, and results already obtained in other projects [1,6].

The projectile's architecture itself needs reforms, as the electrical contact seems to be made only in the tail region of the projectile, not taking advantage of the entire lateral surface of the projectile to conduct current, as can be seen in Fig. 15. General Atomics, the most advanced company in this technology, proposed a geometry for its projectile, encapsulating it in a sabot, in which the contact zone with the rails has the shape of a "U" (see Fig. 15 [17]). Other geometry has already been adopted by other railgun designs.

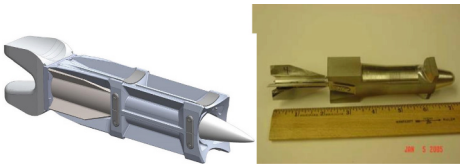

Fig. 15. On the left, the geometry adopted by General Atomics, and on the right, by the EM Gun Project.

Acknowledgements. The authors were supported by Portuguese funds through the Center of Naval Research (CINAV), Naval Academy, Portugal. The author M. Filomena Teodoro was also supported by The Portuguese Foundation for Science and Technology (FCT), through the Center for Computational and Stochastic Mathematics (CEMAT), University of Lisbon, Portugal, project DOI: (https://doi.org/10.54499/UID/04621/ 2025).

References

1. Schoeder, M.K.: An Investigation of the Static Force Balance of a Model Railgun. Monography, Naval Postgraduate School, Monterey, USA (2007)
2. Graneau, P.N.G.: Newtonian Electrodynamics. World Scientific, Singapore (1995)
3. ourselfGadjets, D.I.: Homemade railgun (2013)
4. Persad, C.: Characterization of hypervelocity gouge craters in rail conductors. IEEE Trans. Magn. **33**(1), 197–202 (1997)
5. Pavlov, A.: Improvement of Electromagnetic Railgun Barrel Performance and Lifetime by Method of Interfaces and Augmented Projectiles. Monography, Faculty of California Polytechnic State University, California, USA (2013)
6. PowerLabs: Powerlabs rail gun 2.0 research! (2010). http://www.powerlabs.org/railgun.html. Accessed 20 Apr 2026
7. Maniglia, J.: Design, fabrication, and testing of an eletromagnetic rail gun for the repetead testing and simulation of orbital debris impacts (2013). http://digitalcommons.calpoly.edu/aerosp/. Accessed 20 Apr 2026
8. Bauer, D.P.: Achieving high efficiency with conventional railgun launchers. IEEE Trans. Magn. **31**, 263–266 (1995)
9. Bauer, D.P.: A novel railgun launcher design. IEEE Trans. Magn. **31**, 267–272 (1995). https://api.semanticscholar.org/CorpusID:111118679
10. Herald, T.S.M.: Us navy's new destroyer zumwal will test fire futuristic eletromagnetic railgun (2015). http://www.smh.com.au/technology/sctech/us-navys-new-destroyer-zumwalt-will-test-fire-the-futuristicelectromagnetic-rail-gun-20151209-gljao4.html. Accessed 20 Apr 2026
11. Bindu., S., et al.: Modelling of a spark gap switch. In: 2012 IEEE 10th International Conference on the Properties and Applications of Dielectric Materials, pp. 1–4. IEEE (2012)
12. Maniglia, J.: Design, Fabrication, and Testing of an EMR Gun based Orbital Debris Impact Testing Platform. Faculty of California Polytechnic State University, California, USA, Monography (2013)
13. Atomics, G.: General atomics team powers navy rail gun to new world record (2013)
14. Wendling, M.: Retificadores. Universidade Estadual Paulista, São Paulo, Brasil (2025). http://www2.feg.unesp.br/Home/PaginasPessoais/ProfMarceloWendling/3---retificadores.pdf. Accessed 20 Apr 2026
15. Sampaio, P., Gatta, M., Teodoro, M.F.: Studying of the operation of a railgun system: a theoretical approach. Mathematics (2026)
16. Sampaio, P., Gatta, M., Teodoro, M.F.: Investigating of the operation of a railgun system: experimental approach. In: Machado, J.E.A. (ed.) Lecture Notes in Mechanical Enginneering. Springer (To Appear)
17. Atomics, G.: Projectile development (2016). http://www.ga.com/railgunprojectile-development. Accessed 20 Apr 2026